Evaluation of Cross-frame Designs for Highly Skewed Steel I-Girder Bridges

MATIJA RADOVIC AND JENNIFER MCCONNELL
University of Delaware, Newark DE

Proceedings of 31st International Bridge Conference, Pittsburg, USA. IBC 14-47

KEYWORDS: Cross-frame design, skewed bridges, I-girder, capacity, lateral bending.

ABSTRACT: Cross-frames are known to be critical secondary members in steel I-girder bridges and it is known that these members become more important in highly skewed bridges. However, precise quantification of this effect is lacking. This study contributes towards addressing this need by investigating twelve bridge FEMs with varying cross-frame designs, cross-frame layouts, and bridge skew angles. Variations in cross-frame as well as vertical and lateral bending flange stresses are then evaluated.

INTRODUCTION

Cross-frames are known to be critical secondary members in steel I-girder bridges, which are a ubiquitous configuration of highway bridges in many parts of the US, and in the eastern US in particular. Cross-frames play important roles in providing lateral bracing by reducing the unbraced length of flanges in compression and in assisting in load distribution between girders. It is also known that as bridge skew increases, the role of cross-frames becomes more significant. However, the design and behavior of cross-frames is not a topic that has been well quantified, particularly for skewed and curved bridges.

The research to date has revealed several interesting findings concerning girder stresses in skewed bridges. Specifically, it was shown by Ozgur (2011) that the larger the bridge skew is, the larger the lateral load transfer becomes, influencing bottom flange lateral bending stresses. Krupicka and Poellot (1993) investigated the effects of cross-frames on girder stresses and found that increases in unwanted stiffness in primary members (girders) due to location and stiffness of secondary members (cross-frames) often can occur near skewed supports. If cross-frames are designed such that their stiffness approaches or exceeds that of the girders they can provide "nuisance stiffness" that can induce stresses in the girder's bottom flange that are not typically accounted for. McConnell et al. (2014a) showed that bridge skew and cross-fame placement significantly influence bottom flange lateral bending stress in steel I-girder bridges and confirmed that one means to reduce the bridge transverse stiffness is to use staggered cross-frame configurations. By using this type of cross-frame placement, cross-frame forces are reduced at the expense of increased lateral bending stresses in bottom flange.

On the other hand, concerning cross-frame stresses, Bishara and Elmir (1990) found that the higher the skew angle, the higher the maximum forces that is induced in the cross-frame members. More specifically, McConnell et al. (2013) found through field testing of two skewed I-girder bridges with differing skews that, not only do the cross-frame forces increase with increasing skew, but that these forces can be significantly larger than the girder stresses in highly-skewed structures. Additionally, in evaluating the cross-frame stresses in different cross-frame members, it has been suggested that the diagonal members of K-frames are exposed to significantly lower stresses than the diagonal members of X-frames (Steel Bridge Design Handbook-Bracing System Design, 2012).

Thus, while research such as the works cited above provide insight into the influences of cross-frame designs and skew on the response of both the girder and cross-frame behavior in skewed steel I-girder bridges, additional research continues to be needed in order to provide bridge engineers with quantified information that be used for design and rating of this bridge type. The objectives is to investigate the effects of bridge skew and cross-frame placement on bottom flange lateral bending stresses and cross-frame stresses as these parameters are varied in a parametric finite element analysis (FEA) study based

This paper was originally presented at the 31st Annual International Bridge Conference®, in Pittsburgh, PA (USA), June 8-12, 2014

on a representative bridge that has been field tested and FEA has been validated as accurate in prior research (McConnell et al 2014b, Michaud 2011). This bridge is referred to as Bridge 7R and the details of this bridge are given in the following section. Next, the methodology used in the FEA and the rationale used for creating the parametric suite of twelve finite element models (FEM) is described. The parametric suite consists of all possible combinations of two different cross-frame configurations (X-frame and K-frame), two different layouts (inline and staggered), and three bridge skews (23°, 43°, 63°) that are based on varying the skew of the physical bridge in 20° increments. Results of these efforts are then described, focusing on trends resulting from variations of these three parameters and a comparison of how the FEA stresses compare to girder and cross-frame capacities.

BRIDGE DESCRIPTION

Bridge 7R was a three-span steel I-girder bridge with a composite concrete deck that was recently subjected to a destructive field and FEA evaluation to assess ultimate capacity prior to its decommissioning. Each of the three spans were simply supported and the span of interested measured 105'-3 9/16" in length. The bridge served consisted of 4 girders spaced 8 ft. on center and was highly skewed, having girders positioned 63 degrees from a tangent to the supports.

All four plate girders were fabricated from A7 steel having a web depth of 60 in. and a web thickness of 3/8 in. The top flange dimensions were 20 x 1 in. for the exterior girders and 18 x 7/8 in. for the interior girders. The effective dimensions of the bottom flanges at mid-span, including the cover plates that existed in this location, were 20 x 3-1/8 in. for the exterior girders and 20 x 2-1/2 in. for the interior girders. The web was stiffened with double-sided transverse stiffeners on the interior girders and single-sided transverse stiffeners and single-sided longitudinal stiffeners on the exterior girders. The composite 8 in.-thick concrete deck and 2 in. haunch were connected to the girder with shear connectors.

K-frames were spaced at 20 ft. along the length of the girders, with the first cross-frame being offset 22.5 ft. from the supports. These were composed of 4"x 3 ½"x 3/8" angles and connected to gusset plates, with four bolts at the end of each member, which were in turn bolted to transverse stiffeners welded to the girders. Additionally, end diaphragms were used to connect the girders at each end of the member. The diaphragms were steel I-sections of equal depth to the girders.

FEA MODELING

This section describes the modeling techniques used to create the FEM of Bridge 7R, which serves as the base for the parametric study as well as all other parametric models. All structural components were modeled using a relatively fine mesh of reduced-integration shell elements using the commercial software Abaqus, v.6.11. Longitudinal and transverse deck reinforcement was model using a built-in function in the finite element software. Full composite action between the reinforced concrete deck and the steel girder was developed by using a beam-type multipoint constraint that assures nodal compatibility between the girder top flange and the deck at these locations. The cross-frame-to-girder connection is modeled by merging nodes on the cross-fames and transverse stiffeners serving as connection plates; merged nodes are also used to connect the connection plates, web, and flanges. A view of the mesh of this structure is shown in Fig. 1.

Given the loading considered herein was limited to service level loadings, all material was modeled as linear-elastic. The concrete was given an assumed modulus of elasticity of 3,834,000 psi (4.0ksi compressive strength) and a Poisson's ratio of 0.2. Steel was given a modulus of elasticity of 29,000 ksi and a Poisson's ratio of 0.32.

Preliminary analysis showed that that due to the skew of the bridge alignment, the torsional stresses within the structure were significant enough to cause uplift at some nodes in the acute corners of the bridge. Since there is no physical mechanism to resist this upward movement in the bearings, the boundary conditions of the model accurately represent this condition by using gap elements. The loading was a standard AASHTO HS-20 truck loading (AASHTO 2012), consisting of a front axle of 8 kips spaced fourteen feet from the two

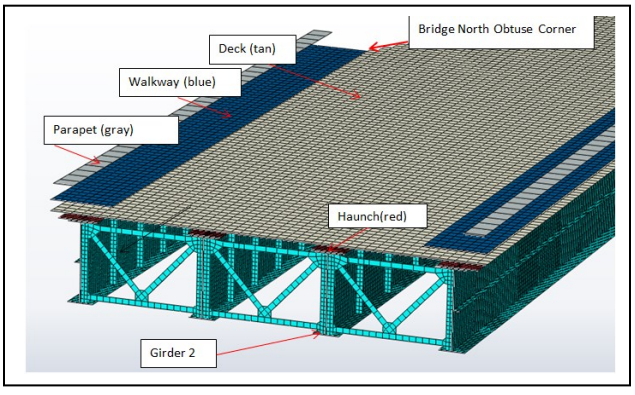

Figure 1. FEM of Bridge 7R (Steel Elements In Aqua; All Other Elements As Noted)

rear axles, each 32 kips, spaced fourteen feet apart. The transverse location of the truck placed the outer line of wheels 1 ft. from the edge of the sidewalk which places the truck above Girder 2 (G2). The longitudinal position of the truck load was simulated with a series of static load cases which varied in position to represent a truck traveling across the length of the bridge. This loading procedure allowed the varying effects of the moving load to be efficiently assessed as the load position causing the maximum force effect in the girders and cross-frames could not be intuitively known with certainty. The loading also included self-weight of all elements.

Linear-elastic, static analysis assuming elastic material properties and geometric linearity was used in the FEA. These assumptions are justified based on the level of loading applied in these models, which were proven to be within the elastic range of all elements, and prior studies showing that the influence of geometric non-linearity is trivial for the range of loading considered here.

DESCRIPTION OF PARAMETRIC STUDY

Bridge 7R, described above, serves as the basis for the parametric study. All aspects of this bridge (girder and concrete dimensions, material properties, etc.) except for skew and cross-frame design are constant in all parametric models. Then, all combinations of two common cross-frame configurations (K-frames and X-frames), two common cross-frame layouts (inline and staggered), and three skew angles (23°, 43° and 63°) are considered to form a parametric suite of 12 models. The four possible combinations of cross-frame parameters are referred to herein as X-frame Inline, X-frame Staggered, K-frame Inline, and K-frame Staggered. The three skew angles are based on altering the skew of the physical bridge (63°) in 20° increments in order to cover the practical range of skews through a minimum of 20° since this is a typical lower bound for when special design considerations are made due to the presence of skew. The capacity of the physical girders to resist design moments in a bridge with a lower skew, and thus higher live load moment distribution factor, were checked and found to be acceptable.

The cross-frame design for the K-frame models was identical to the member sizes, geometry, and spacings used in the physical bridge. The cross-frame design for the X-frame models was based on the same member sizes and spacing, but revising the geometry to form an X configuration. Similarly, the cross-frame layout for the inline models at 63° was the same as in the physical bridge, with cross-frames spaced at 20 ft. along the length of the bridge with the e exception of the first cross-frame lines adjacent to the abutments which is a variable distance of 25 ft. or less. The configuration was maintained to the extent possible for the differing skew angles, where a cross-frame spacing of 21.5 ft. is used along the length of the bridge with the e exception of the first cross-frame lines adjacent to the abutments which is a variable distance of 25 ft. or less. The cross-frame layout for the staggered models was based on original plans of Bridge 7R where the first cross-frame line was 22.5 ft. from the supports for the exterior girders. In the staggered models the first cross-frame from the abutment was 22.5 ft. from the support line for all girders. Then the spacing between the cross-frames was kept the same as used in the inline models for the corresponding skews (20 ft. for 63° and 21.5 ft. for 43° and 23°). This method resulted in stagger distances between cross-frames of 4.8 ft. for the 63° skew models, 8 ft. for the 43° skew models, and 5.6 ft. for the 23° skew models.

DATA ANALYSIS METHODOLOGY

Maximum magnitudes of compressive and tensile stresses in the cross frames, the locations of these stresses, and the location of the applied load producing these stresses were recorded during post-processing. These stresses were then compared to corresponding tensile and compressive capacities computed per the American Institute of Steel Construction, Steel Construction Manual (AISC, 2010) and then converted to stress capacities in order to readily compare the capacities with the FEA output. This data is summarized below in Table 1, with the governing tensile (ϕF_t) and compressive (ϕF_c) stress capacities for each member listed in bold font. These calculations assume a yield stress of 36 ksi and an ultimate stress of 55 ksi.

Two critical girder locations were selected for analyzing girder stresses in the longitudinal direction. These stresses are referred to as bending stresses in the discussion that follows. The first critical girder location was at the mid-span of G2. This is theoretical location of maximum vertical bending stress in the bottom flange. The second critical location is the north obtuse corner of the bridge, where the end diaphragm frames into the girder. This is the observed location of the maximum lateral bending stress. In addition to tabulating total stress results, the vertical and lateral bending components were calculated by solving the following system of equations.

$$V_B + L_B = T_1 \qquad \text{Equation (1)}$$

$$V_B - L_B = T_2 \qquad \text{Equation (2)}$$

Table 1. Tensile and Compressive Stress Capacity for Cross-frame Members

		4x 3½ x ⅜ (Diagonal)		4x 3½ x ⅜ (Bottom Chord)	
		X-frame	K-frame	X-frame	K-frame
Tension Calculations	ϕf_{t_f} (ksi)	33.0	33.0	33.0	33.0
	ϕf_{t_y} (ksi)	32.4	32.4	32.4	32.4
	ϕF_t (ksi)	**32.4**	**32.4**	**32.4**	**32.4**
Compression Calculations	Unbraced length (in.)	45	58	83	40
	$Q\lambda_{cz}$	0.53	0.68	0.97	0.47
	kl/r_z	46.9	60.5	86.6	41.7
	ϕF_c (ksi)	**23.2**	**20.4**	**16.0**	**24.3**

In Equations 1 and 2, V_B is the vertical bending stress, L_B is the lateral bending stress, and T_1 and T_2 are the two total stress values obtained from the FEA at the outer edges of the flange cross-section. Figure 2 conceptually demonstrates how the vertical and lateral bending forces sum to produce these results. At present, the total stress will be compared to the assumed yield stress of 36 ksi, which is the tensile and local buckling resistance. Calculation of the allowable lateral bending stresses, which may be less than the yield stress, is planned for future work.

RESULTS

CROSS-FRAME RESULTS: Table 2 shows the maximum compressive and tensile cross-frame stresses for the twelve parametric models and Figures 3 and 4 display these trends graphically. As was expected based on prior research on this topic (see Introduction), when increasing the bridge skew for any of the four cross-frame designs, both the compressive and tensile cross-frame stresses were generally increased by a significant margin. Specifically, the largest percent increase in tensile stress was 194%, which occurred in the X-frame Inline model; the largest percent increase in compression stress was 221%, which occurred in the K-frame Staggered model (Figure 4). The largest increase in stress magnitude was a change in tensile stress of 7.2 ksi, which occurred in the K-frame Inline model. Additionally, the largest increase in compressive stress magnitude was 4.8 ksi, which also occurred in the K-frame Inline model. On the other hand, the lowest cross-frame stresses in both tension (4.3 ksi) and compression (2.4 ksi) as well as the least sensitivity to variations in compression stress with variation in skew were recorded in the X-frame Staggered model. The least sensitivity to tension stress with variable skew occurred in the K-frame Staggered model.

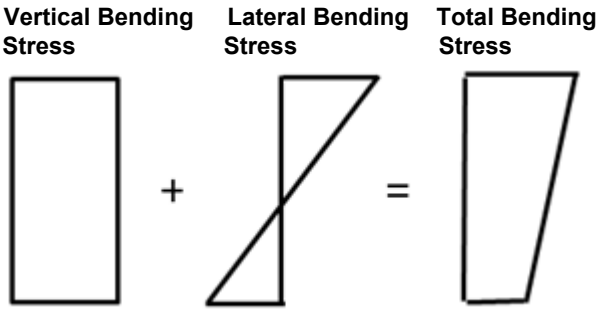

Figure 2. Effect of Biaxial Bending of the Bottom Flange

Table 2. Maximum Compressive and Tensile Cross-frame Stresses and Their Locations (BC = Bottom Chord, LD = Left Diagonal and RD = Right Diagonal)

		CROSS-FRAME DESIGN			
ACTION	BRIDGE SKEW	X-FRAME STAGGERED	X-FRAME INLINE	K-FRAME STAGGERED	K-FRAME INLINE
TENSION (KSI)	23°	4.4 (RD)	4.7 (LD)	8.0 (BC)	10.3 (BC)
	43°	5.5 (BC)	9.0 (BC)	10.8 (BC)	17.2 (BC)
	63°	7.5 (BC)	9.2 (BC)	8.3 (BC)	17.5 (BC)
COMPRESSION (KSI)	23°	2.5 (RD)	2.8 (LD)	3.7 (LD)	6.1 (LD)
	43°	4.3 (RD)	5.7 (RD)	6.7 (BC)	8.1 (BC)
	63°	3.8 (RD)	5.6 (LD)	8.1 (BC)	10.9 (LD)

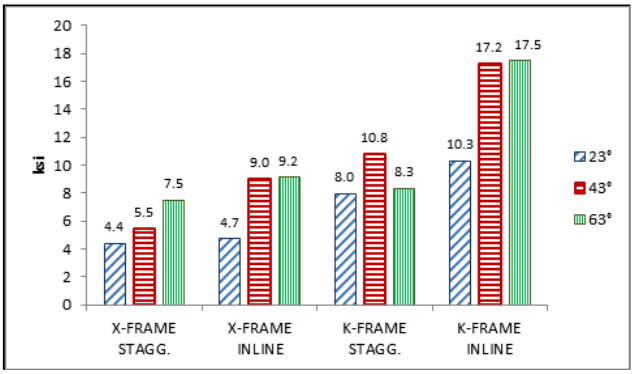

Figure 3. Maximum Tensile Cross-frame Stresses

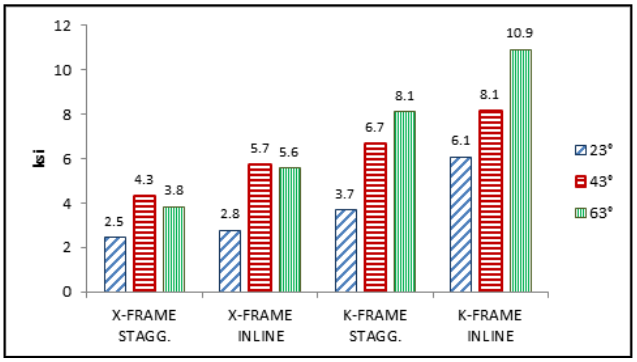

Figure 4. Maximum Compressive Cross-frame Stresses

It is known that placing cross-frames in discontinuous lines will reduce the transverse stiffness of the bridge. Theoretically, this will cause a decrease in cross-frame forces, but increase in flange lateral bending stress. Accordingly, an inline cross-frame configuration will induce more forces in the cross-frames compared to a staggered cross-frame configuration. The results shown in Table 2 validate that this is true for the models considered herein, where the staggered model exhibits a lower peak cross-frame stress than the corresponding inline model in all cases. This stress difference is as large as 9.2 ksi, or 110%, in the 63° K-frame models.

The results in Table 2 and Figures 3 and 4 also demonstrate that cross-frame configuration plays a role in increasing or decreasing cross-frame forces. Specifically, in all cases the K-frame configuration has significantly greater peak stresses than the corresponding X-frame configuration. The greatest difference in this regard in terms of stress magnitude is 8.3 ksi, which occurs in the 63° inline models experiencing tension. In terms of percent difference, the greatest difference between the X-frame and K-frame models is 120%, which occurs in the 23° staggered models experiencing tension.

Results also showed that bridge skew changes the distribution of stress within cross-frame members. For example, at low bridge skew (23°) the location of the maximum tensile stresses in X-frame members is located in the diagonals, while at larger skews (43° and 63°) the location of the maximum tensile stress is located in the bottom chords. For K-frames at low bridge skews (23°), the peak tensile stress occurs in the bottom chord while the peak compressive stress occurs simultaneously in the diagonal of the same cross-frame. However, at larger skews (43° and 63°), the locations of both the peak compressive and tensile stresses are the bottom chord. More specifically, they are located on the opposing sides of the connection plate at the mid-length of the bottom chord, where Figure 5 shows the maximum compressive (8124 psi) and tensile (8343 psi) stresses that are concurrently occurring during the same load case in the same bottom chord K-frame Staggered model. The load case producing these maximum compressive and tensile forces is where the front axle of HS-20 vehicle is a longitudinal distance of 66 ft from north abutment. Additionally, the figure shows double curvature bending of this bottom chord.

Table 2 also shows that cross-frames compressive stresses are generally smaller than cross-frame tensile stresses. The maximum compressive stress (10.9 ksi) was recorded in the left diagonal member of the K-

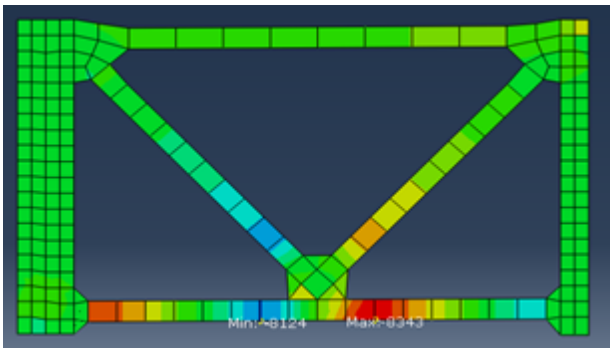

(a) Front View

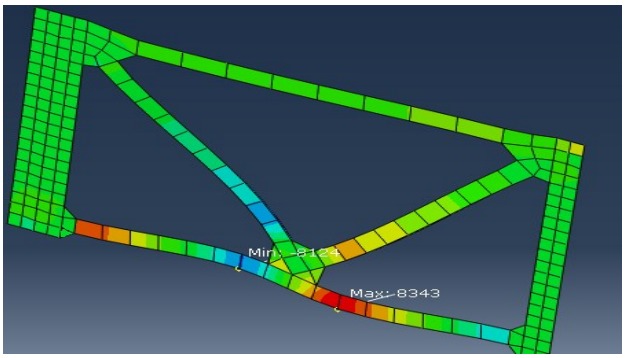

(b) Isometric View Showing Deflected Shape

Figure 5. Location Of Maximum Tensile And Compressive Stress At Bottom Chord Of K-Frame Cross-Frame At Bridge Skew Of 63° (Where Blue Represents Compression And Red Represents Tension)

frame Inline model at 63° skew. However, it is also known that these members will have less capacity in compression (see Table 1). Thus, Figure 6 shows demand vs. capacity ratios that were computed for all cross-frame models by taking the ratios between the data in Tables 1 and 2. When viewed from this perspective, there is not a significant difference in the significance of the tension forces and the compression forces, with the demand to capacity ratios ranging between 11% and 54% for all cases. Figure 6 also shows the intuitive result that the demand to capacity ratio typically increases as skew increases. Furthermore, Figure 6 shows that the X-frame Staggered model has the lowest percent of demand vs. capacity ratio for both tension (23%) and compression (16%), for the most critical skew angle (63°). These values are significantly less than the K-frame Inline model, which exhibits the highest demand vs. capacity ratios for both tension (54%) and compression (53%).

BOTTOM FLANGE RESULTS: Table 3 shows the maximum vertical bending stresses (V_B) at two critical girder locations (at mid-span and at north obtuse

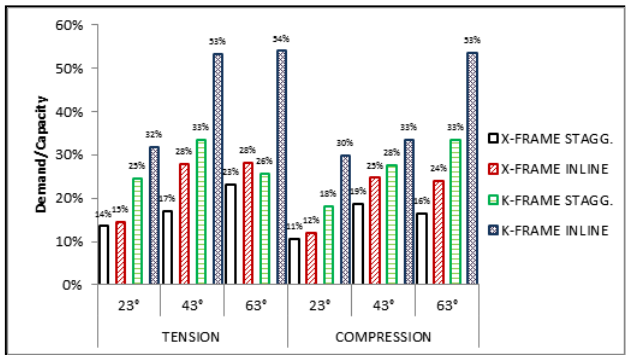

Figure 6. Demand vs. Capacity Ratios for Cross-frame Members

Table 3. Maximum Bottom Flange Vertical Bending Stresses at Two Critical Locations (ksi)

		CROSS-FRAME DESIGN			
LOCATION	BRIDGE SKEW	X-FRAME STAGGERED	X-FRAME INLINE	K-FRAME STAGGERED	K-FRAME INLINE
MID-SPAN	23°	9.2	9.1	9.3	9.2
	43°	8.3	8.0	8.3	8.0
	63°	7.4	7.1	7.4	7.1
OBTUSE CORNER	23°	0.8	0.8	0.8	1.5
	43°	0.4	0.2	0.4	0.3
	63°	1.2	1.0	1.1	1.0

corner of the bridge). Figure 7 presents this same data graphically. It is known that the theoretical location of maximum vertical bending stress in a simply supported bridge girder is at mid-span. The FEA results show that for the smallest bridge skew angle (23°), this theoretical vertical bending stress is the dominate type of flange stress, and the vertical bending stress at flange at the mid-span, is larger than any type of bottom flange stress the obtuse corner. Results show that as the bridge skew increases, the vertical bending stresses at mid-span decreases regardless of the cross-frame configuration or placement. At the same time as the bridge skew significantly increases the lateral bending stresses at the obtuse corner (Figure 8). The largest difference in lateral bending stresses was detected at K-frame Inline model where the difference in lateral bending stresses at 23° vs. 63° skew was 10.7 ksi or 565%. Additionally, for the larger skew angles (43° and 63°) the lateral bending stress at the obtuse corner becomes the dominant bottom flange stress type, becoming even larger than the vertical bending stress at mid-span.

The majority of the bending at the obtuse corner of the bridge is attributed to lateral bending, as seen by comparison of the lateral bending stresses reported in Table 4 relative to the vertical bending stresses reported in Table 3. Figure 8 presents the data in

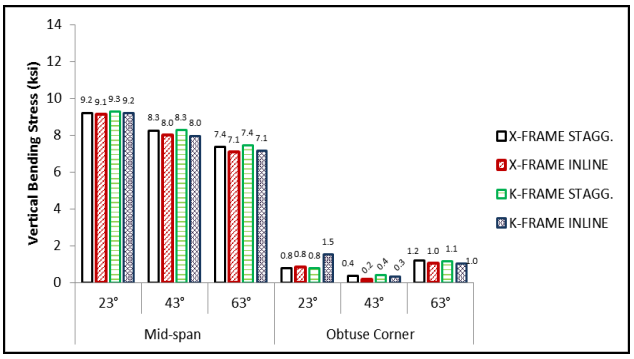

Figure 7. Maximum Vertical Bending Stresses at Two Critical Locations

Table 4. Maximum Lateral Bending Stresses at Two Critical Locations (ksi)

		CROSS-FRAME DESIGN			
LOCATION	BRIDGE SKEW	X-FRAME STAGGERED	X-FRAME INLINE	K-FRAME STAGGERED	K-FRAME INLINE
MID-SPAN	23°	0.5	0.1	0.5	0.1
	43°	0.7	0.3	0.6	0.2
	63°	1.9	0.2	1.1	0.2
OBTUSE CORNER	23°	5.7	5.9	5.7	2.3
	43°	9.9	9.2	9.8	11.2
	63°	13.7	13.1	13.3	13.0

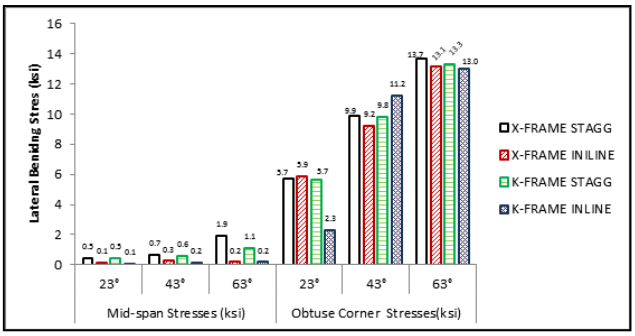

Figure 8. Maximum Lateral Bending Stresses at Two Critical Locations

Table 4 graphically, which can be considered relative to the vertical bending data shown in Figure 8. It is also interesting to note that the magnitude of the lateral bending stresses at the obtuse corner of the bridge is fairly consistent for the various cross-frame designs. The lateral bending at this location is primarily attributed to the end diaphragm that frames directly into the girders at this location. Since the diaphragm stiffness is approximately the same as the girders', it attracts significant stress. As the skew increases, the diaphragm stress increases, which in turn increases the lateral bending stress in the girders. In contrast, the results in Table 4 show that lateral bending stress at the mid-span is relatively small in all cases (maximum of 1.9 ksi) and less than 1.0 ksi for all models with skew of 43° or less. The maximum lateral bending stress (13.7 ksi) at the obtuse corner is 7.2

times the maximum lateral bending stress at the mid span of the bridge (1.9 ksi). Both of these maximums occur in the same model, the X-frame Staggered model. Furthermore, this maximum lateral bending stress at the obtuse corner is 1.5 times larger than the maximum vertical bending stress at mid-span for the same model (9.2 ksi).

CONCLUSION

The results of this study suggest that X-frame Staggered model is the most efficient cross-frame design for the models considered herein, with evidence to suggest that this may be a general trend. This conclusion is based in part on the data presented in Table 2, where it is shown that this cross-frame design results in the lowest cross-frame forces, which are as much as 12% less than (for 23° skew) to 65% less than (for 63° skew) maximum stresses in other cross-frame designs. Figure 6 has also shown that the X-frame Staggered models also result in the lowest demand to capacity ratios for the cross-frame stresses. As discussed above, this result occurs because of the decreased stiffness of this cross-frame design and it would be expected that this decreased stiffness would lead to greater lateral bending stresses in the girder. This theoretical expectation was revealed to be true in the FEA results presented in Table 4, where the staggered cross-frame designs exhibited greater lateral bending than their inline counterparts, especially at the mid-span location when the results are considered in terms of percent difference. However, this study showed that these mid-span lateral bending stresses are less than 2 ksi. The difference in magnitude of lateral bending stress between corresponding models with staggered and inline cross-frames is greatest at the obtuse corner of the bridge, with a maximum difference in magnitude of 3.4 ksi.

Thus, these modest increases in stress are deemed to be a worthwhile tradeoff given the reduced cross-frame stresses afforded by a staggered cross-frame configuration. This is especially true when considering that it can be observed via comparison of the data in Tables 1 and 2 that the cross-frame stresses are generally much closer in magnitude to their limiting stresses than the girder stresses are to their yield stress. However, it is acknowledged that the lateral buckling capacity of the bottom flanges should be calculated prior to making a final recommendation on this matter. The conclusion that the X-frame Staggered configuration is also the best design for these parametric models is also based on the fact that the most critical location for lateral bending stresses is not at mid-span but at the north obtuse corner of the bridge. Here the difference in lateral bending at the most critical skew angle (63°) is within 5% for the four cross-frame designs.

In contrast, the worst performance in terms of the metrics evaluated in this work, was observed in the K-frame Inline model. In this model, the compressive cross-frame forces were 185% larger than the corresponding forces in the X-frame Staggered model at 63° skew , while the reduction in lateral bending stress at the obtuse corner was only 5% better than this same model. Finally, results show that both cross-frame compressive and tensile capacity and bottom flange yielding and local buckling resistance were sufficient for all models. Lateral buckling resistance of the bottom flange will be computed in future work to complete this assessment.

REFFERENCES

Ozgur, C.” Influence Of Cross-Frame Detailing On Curved And Skewed Steel I-Girder Bridges”, Doctoral Dissertation, Georgia Institute of Technology. p.21 (2011)

Krupicka, G., and Poellot, B. “Nuisance Stiffness,” Bridgeline, p.3, 4(1), HDR Engineering, Inc., (1993)

McConnell, J., Radovic, M., and Ambrose, K. “Cross-Frame Forces in Skewed Steel I-Girder Bridges: Field Measurements and Finite Element Analysis”, University of Delaware Center for Bridge Engineering, Final Report to Delaware Department of Transportation (2014a)

Michaud, K “Evaluating Reserve Bridge Capacity Through Destructive Testing of a Decommissioned Bridge” p.95 , Master Thesis, University of Delaware,(2011)

Hartman, A. S., Hassel, H. L., Adams, C. A., Bennett, C. R., Matamoros, A. B., and Rolfe, S. T. Transportation Research Record: Journal of the Transportation Research Board, 2200(-1), p.62-68. (2010)

Bishara, A. G., and Elmir, W. E. Journal of Structural Engineering, 5 116-20 (1990)

McConnell, J., Ambrose, K., and Radovic, M. “Cross-Frame Forces in Skewed Steel I-Girder Bridges: Field Testing and Applications to System-Capacity”, 2013 ASCE / SEI Structures Congress, Pittsburgh, PA, (2013)

Federal Highway Administration “Bracing System Design”, Steel Bridge Design Handbook, Washington D.C (2012)

McConnell, J.; Chajes, M.; and Michaud, K. ASCE Journal of Structural Engineering, under review. (2014b)

Ross, J. H. “Evaluating Ultimate Bridge Capacity Through Destructive Testing of Decommissioned Bridges.” Master Thesis. University of Delaware. (2007)

American Institute Of Steel Construction Steel Construction Manual 14th Edition. American Institute of Steel Construction Officials. (2010)

AASHTO, AASHTO LRFD Bridge Design Specifications, 5th Edition, American Association of State Highway and Transportation Officials, Washington, DC. (2012)